# Supplementary Information: Using a Wald model to study time perception in intervals with varying proportions of cognitively demanding and idle phases

**Álvaro Garrido-Pérez, Amrapali Pednekar, Pieter Simoens, and Yara Khaluf**

**Note.** The references cited in this document correspond to those listed in the main article.

## Supplementary Methods

### Subjective difficulty assessment

After the reproduction stage of each trial, participants were asked:

*"Please indicate how difficult it was to choose a lottery in the experiment round you just completed"*

Participants responded on a 5-point Likert scale with the following options:

- ☐ Very easy
- ☐ Easy
- ☐ Medium
- ☐ Hard
- ☐ Very hard

### Instruction comprehension checks

Every participant had to complete the following comprehension check after receiving the instructions and before starting the experiment. Participants had 3 attempts to answer each question correctly and they could always read the relevant instruction section again before answering. The correct answers are indicated with a green check mark.

#### *Question 1*

Imagine that you choose the Left lottery in the example shown in the image below. Imagine as well that this lottery is drawn from the *bag of selected lotteries* at the end of the experiment. If you play the lottery, what is the probability of earning Ghentian dollars? And how many Ghentian dollars could you potentially earn?

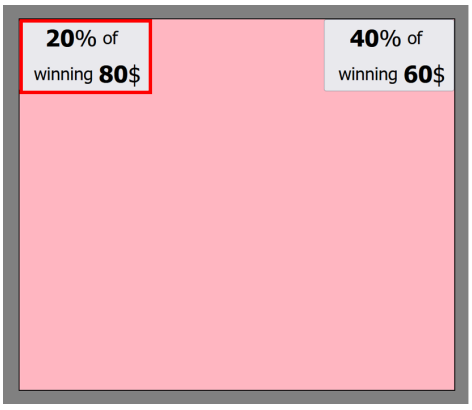


- ☐ I could earn 40 Ghentian dollars with a probability of 60%
- ☐ I could earn 60 Ghentian dollars with a probability of 40%

- ☐ I could earn 80 Ghentian dollars with a probability of 20% ✓
- ☐ I could earn 20 Ghentian dollars with a probability of 80%

***Question 2***

Imagine that you choose the Right lottery in the example shown in the image below. Imagine as well that this lottery is drawn from the *bag of selected lotteries* at the end of the experiment. If you play the lottery, what is the probability of getting 0 Ghentian dollars?

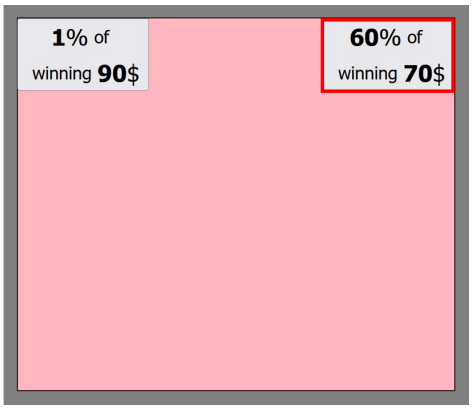


- ☐ 60%
- ☐ 70%
- ☐ 30%
- ☐ 40% ✓

***Question 3***

For a given round, if you have not selected a lottery before the deadline, then:

- ☐ You can still pick a lottery in that round. However, if that lottery is one of the 8 selected lotteries at the end of the experiment, you will only obtain half of the lottery's outcome that you would have obtained, had you not missed the deadline ✓
- ☐ You cannot pick a lottery in that round
- ☐ You can still pick a lottery in that round and there are no consequences for missing the deadline

***Question 4***

What time interval should you reproduce after each round?

- ☐ Regardless of whether I miss the deadline or not, from the moment the lotteries appear until the moment I choose a lottery (which is equal to the *decision time*)
- ☐ Regardless of whether I miss the deadline or not, the amount of time that the lotteries were displayed. If I don't miss the deadline, then it will be equal to *decision time* + *waiting time*. If I miss the deadline, then it will only be equal to the *decision time* ✓
- ☐ Regardless of whether I miss the deadline or not, from the moment I choose a lottery until the moment the lotteries disappear (which is equal to the *waiting time*)
- ☐ Regardless of whether I miss the deadline or not, from the moment the lotteries appear until the moment the black cross disappears

### Gambles used in the duak-task stage

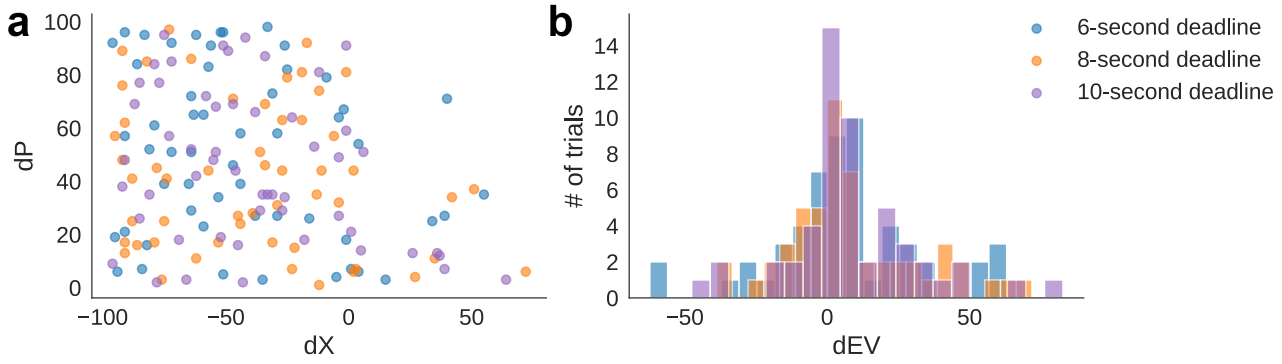


**Figure S1.** Gamble attributes. (**a**) Distribution of gambles in the dX-dP space, where dX represents the payoff difference and dP the probability difference between the safer and riskier lotteries. The safer lottery is defined as the option with the higher probability, while the riskier lottery has the lower probability. Colours correspond to the deadline conditions assigned to each gamble (6, 8, or 10 seconds). (**b**) Histogram of gambles based on the difference in expected value (dEV) between the safer and riskier lotteries, separated by deadline condition. An optimal decision-maker should select the option with the highest expected value; therefore, gambles with dEV values near zero are expected to be harder.

### Drift-diffusion model

The drift-diffusion model and its priors were specified as follows:

$$
\begin{aligned}
a_{\text{ddm}} &\sim \mathcal{U}(0.5, 3.5) \\
t_{\text{ddm}} &\sim \mathcal{HN}(0, .3) \\
v_{\text{x}} &\sim \mathcal{HN}(0, 3) \\
v_{\text{p}} &\sim \mathcal{HN}(0, 3) \\
v_{\text{ev}} &\sim \mathcal{HN}(0, 3) \\
v_{\text{ddm},t} &= v_x \, \text{dX}_t + v_p \, \text{dP}_t + v_{ev} \, \text{dEV}_t \\
\text{RT}_t &\sim \text{WFPT}(v_{\text{ddm},t}, a_{\text{ddm}}, t_{\text{ddm}}, .5)
\end{aligned}
$$

Where $\text{RT}_t$ is the reaction time at trial $t$ and $\text{dX}_t$, $\text{dP}_t$ and $\text{dEV}_t$, are the differences in payoff, probability and expected value of the lotteries in trial $t$, respectively. The function *WFPT(·)* denotes the Wiener First Passage Time distribution. The prior distributions were chosen to match the range of parameter estimates reported in a previous study that employed the same DDM for a similar task[26].

### Hierarchical Bayesian Wald models

A graphical representation of the full Wald model can be seen in Fig. S2. The full model and its priors were specified as follows:

$$
\begin{aligned}
&\mu_{\beta_0} \sim \mathcal{N}(0, .5)\,;\ \sigma_{\beta_0} \sim \mathcal{HN}(0, .5)\\
&\mu_{\beta_1} \sim \mathcal{N}(0, .5)\,;\ \sigma_{\beta_1} \sim \mathcal{HN}(0, .5)\\
&\mu_{\beta_2} \sim \mathcal{N}(0, .5)\,;\ \sigma_{\beta_2} \sim \mathcal{HN}(0, .5)\\
&\mu_{v_{\text{wm}}} \sim \mathcal{N}(0, .5)\,;\ \sigma_{v_{\text{wm}}} \sim \mathcal{HN}(0, .5)\\
&\beta_0^i \sim \exp(\mathcal{N}(\mu_{\beta_0}, \sigma_{\beta_0}))\\
&\beta_1^i \sim \exp(\mathcal{N}(\mu_{\beta_1}, \sigma_{\beta_1}))\\
&\beta_2^i \sim \exp(\mathcal{N}(\mu_{\beta_2}, \sigma_{\beta_2}))\\
&v_{\text{wm}}^i \sim \exp(\mathcal{N}(\mu_{v_{\text{wm}}}, \sigma_{v_{\text{wm}}}))\\
&a_{\text{wm},t}^i = \beta_0^i + \beta_1^i\,\text{RT}_t^i + \beta_2^i\,\text{IT}_t^i\\
&\text{ReproT}_t^i \sim \text{Wald}(\mu = \tfrac{a_{\text{wm},t}^i}{v_{\text{wm}}^i}, \lambda = (a_{\text{wm},t}^i)^2, \alpha = t_{\text{wm}})
\end{aligned}
$$

Where $i$ indexes participants and $t$, indexes trials. The function *Wald(·)* denotes the Wald (or Inverse Gaussian) distribution, which in PyMC is parameterized by three parameters: $\mu$, the mean; $\lambda$, which controls the spread of the distribution; and $\alpha$, a shift parameter representing the non-decision time (i.e., $\alpha = t_{\text{wm}}$). We fixed the non-decision time to 250 ms, so $t_{\text{wm}}$ was not treated as a free parameter.

The prior distributions were specified to be weakly informative while constraining reproduced times to positive values. The priors encode plausible assumptions, as demonstrated in Fig. S3.

We also fitted a version of the Wald model (the *simple* Wald model) where the pulse-transfer rate ($\beta_t$) is the same during the decision-making and the idle phases. The simple Wald model was specified as follows:

$$
\begin{aligned}
&\mu_{\beta_0} \sim \mathcal{N}(0, .5)\,;\ \sigma_{\beta_0} \sim \mathcal{HN}(0, .5)\\
&\mu_{\beta_t} \sim \mathcal{N}(0, .5)\,;\ \sigma_{\beta_t} \sim \mathcal{HN}(0, .5)\\
&\mu_{v_{\text{wm}}} \sim \mathcal{N}(0, .5)\,;\ \sigma_{v_{\text{wm}}} \sim \mathcal{HN}(0, .5)\\
&\beta_0^i \sim \exp(\mathcal{N}(\mu_{\beta_0}, \sigma_{\beta_0}))\\
&\beta_t^i \sim \exp(\mathcal{N}(\mu_{\beta_t}, \sigma_{\beta_t}))\\
&v_{\text{wm}}^i \sim \exp(\mathcal{N}(\mu_{v_{\text{wm}}}, \sigma_{v_{\text{wm}}}))\\
&a_{\text{wm},t}^i = \beta_0^i + \beta_t^i\,\text{TT}_t^i\\
&\text{ReproT}_t^i \sim \text{Wald}(\mu = \tfrac{a_{\text{wm},t}^i}{v_{\text{wm}}^i}, \lambda = (a_{\text{wm},t}^i)^2, \alpha = t_{\text{wm}})
\end{aligned}
$$

Where $\text{TT}_t^i$ is the target time of trial $t$ for subject $i$.

Finally, we fitted a version of the Wald model (the *Null* Wald model) where there is no information about the experienced target time. The Null Wald model was specified as follows:

$$
\begin{aligned}
&\mu_{\beta_0} \sim \mathcal{N}(2, .5)\,;\ \sigma_{\beta_0} \sim \mathcal{HN}(0, .5)\\
&\mu_{v_{\text{wm}}} \sim \mathcal{N}(0, .5)\,;\ \sigma_{v_{\text{wm}}} \sim \mathcal{HN}(0, .5)\\
&\beta_0^i \sim \exp(\mathcal{N}(\mu_{\beta_0}, \sigma_{\beta_0}))\\
&v_{\text{wm}}^i \sim \exp(\mathcal{N}(\mu_{v_{\text{wm}}}, \sigma_{v_{\text{wm}}}))\\
&a_{\text{wm},t}^i = \beta_0^i\\
&\text{ReproT}_t^i \sim \text{Wald}(\mu = \tfrac{a_{\text{wm},t}^i}{v_{\text{wm}}^i}, \lambda = (a_{\text{wm},t}^i)^2, \alpha = t_{\text{wm}})
\end{aligned}
$$

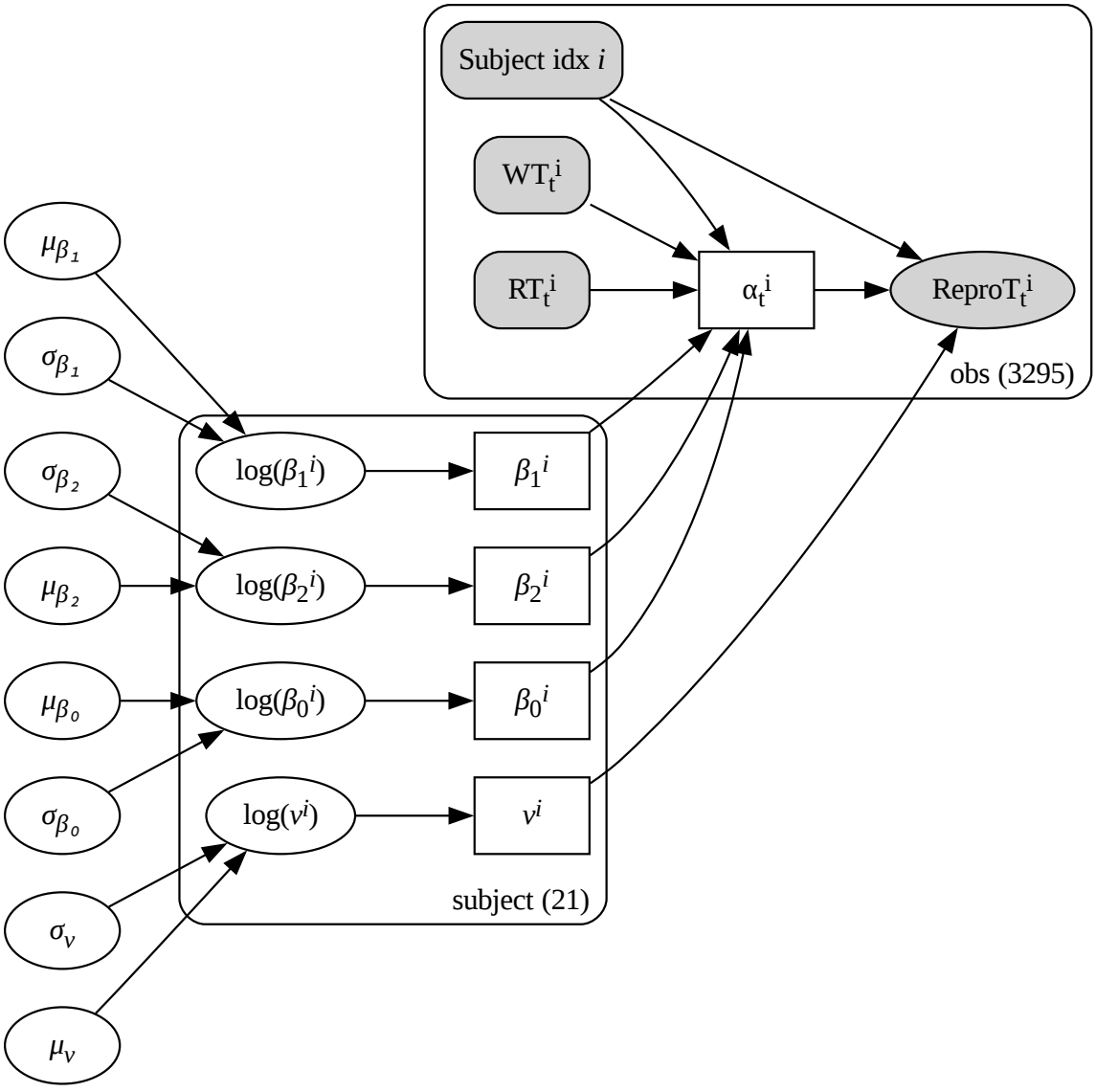


**Figure S2.** Graphical representation of the hierarchical (full) Wald model. Shaded nodes represent observed variables, whereas unshaded nodes represent latent variables. Square nodes indicate variables derived from deterministic operations. Here, a "subject" refers to a participant.

### Hierarchical Bayesian Regression models

The full regression model and its priors were specified as follows:

$$
\begin{aligned}
&\mu_{\beta_0} \sim \mathcal{N}(-.5, .5)\,;\ \sigma_{\beta_0} \sim \mathcal{HN}(0, .5)\\
&\mu_{\beta_1} \sim \mathcal{N}(-.5, .5)\,;\ \sigma_{\beta_1} \sim \mathcal{HN}(0, .5)\\
&\mu_{\beta_2} \sim \mathcal{N}(-.5, .5)\,;\ \sigma_{\beta_2} \sim \mathcal{HN}(0, .5)\\
&\mu_{\sigma} \sim \mathcal{N}(-.5, .5)\,;\ \sigma_{\sigma} \sim \mathcal{HN}(0, .5)\\
&\beta_0^i \sim \exp(\mathcal{N}(\mu_{\beta_0}, \sigma_{\beta_0}))\\
&\beta_1^i \sim \exp(\mathcal{N}(\mu_{\beta_1}, \sigma_{\beta_1}))\\
&\beta_2^i \sim \exp(\mathcal{N}(\mu_{\beta_2}, \sigma_{\beta_2}))\\
&\sigma^i_{\text{ReproT}} \sim \exp(\mathcal{N}(\mu_{\sigma}, \sigma_{\sigma}))\\
&\mu^i_{\text{ReproT},t} = \beta_0^i + \beta_1^i\,\text{RT}_t^i + \beta_2^i\,\text{IT}_t^i\\
&\text{ReproT}_t^i \sim \mathcal{N}(\mu^i_{\text{ReproT},t}, \sigma^i_{\text{ReproT}})
\end{aligned}
$$

As for the Wald model, a version of the regression model (that we termed the *simple regression* model) was also fitted, where the pulse-transfer rate is the same during decision-making and idleness. The simple regression model was specified as follows:

$$
\begin{aligned}
&\mu_{\beta_0} \sim \mathcal{N}(-.5, .5)\,;\ \sigma_{\beta_0} \sim \mathcal{HN}(0, .5)\\
&\mu_{\beta_t} \sim \mathcal{N}(-.5, .5)\,;\ \sigma_{\beta_t} \sim \mathcal{HN}(0, .5)\\
&\mu_{\sigma} \sim \mathcal{N}(-.5, .5)\,;\ \sigma_{\sigma} \sim \mathcal{HN}(0, .5)\\
&\beta_0^i \sim \exp(\mathcal{N}(\mu_{\beta_0}, \sigma_{\beta_0}))\\
&\beta_t^i \sim \exp(\mathcal{N}(\mu_{\beta_t}, \sigma_{\beta_t}))\\
&\sigma^i_{\text{ReproT}} \sim \exp(\mathcal{N}(\mu_{\sigma}, \sigma_{\sigma}))\\
&\mu^i_{\text{ReproT},t} = \beta_0^i + \beta_t^i\,\text{TT}_t^i\\
&\text{ReproT}_t^i \sim \mathcal{N}(\mu^i_{\text{ReproT},t}, \sigma^i_{\text{ReproT}})
\end{aligned}
$$

The prior distributions were once again specified to be weakly informative while constraining reproduced times to positive values. Figure S3 shows the prior predictive distributions of the regression models compared to the observed distribution of reproduced times.

**Prior predictive distributions**

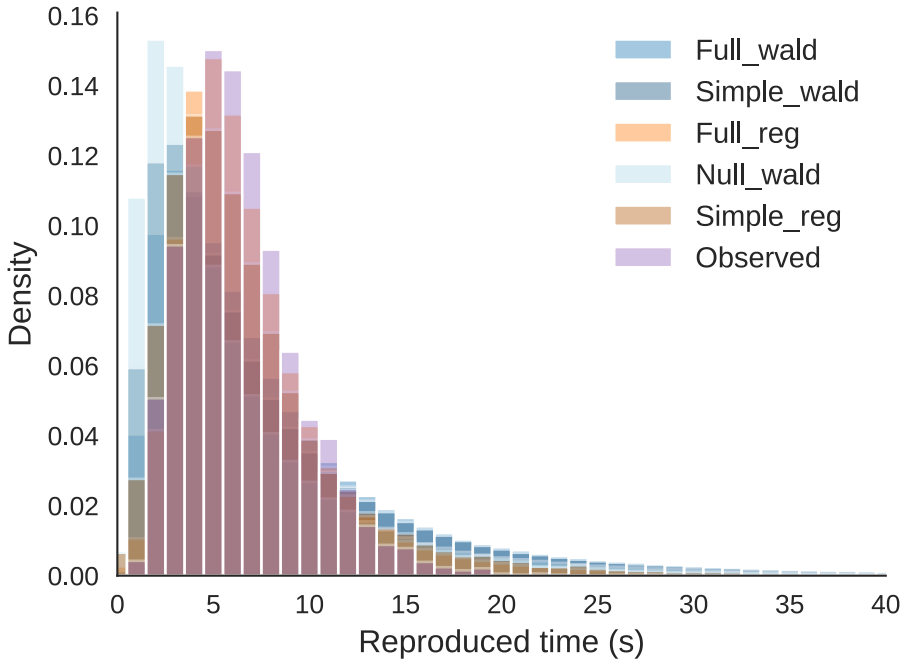


**Figure S3.** Prior predictive distributions compared to observed distributions of reproduced times. Histograms for the Wald and regression models were generated by drawing 500 samples from their prior predictive distributions.

## Wald model Posterior Predictive Check

The posterior predictive check consists of comparing the observed distribution of reproduced times with a distribution of simulated reproduced times (known as the posterior predictive distribution) generated using parameter values drawn from the posterior distribution. As shown in Fig. S4, the posterior predictive and observed distributions match closely, indicating a good fit.

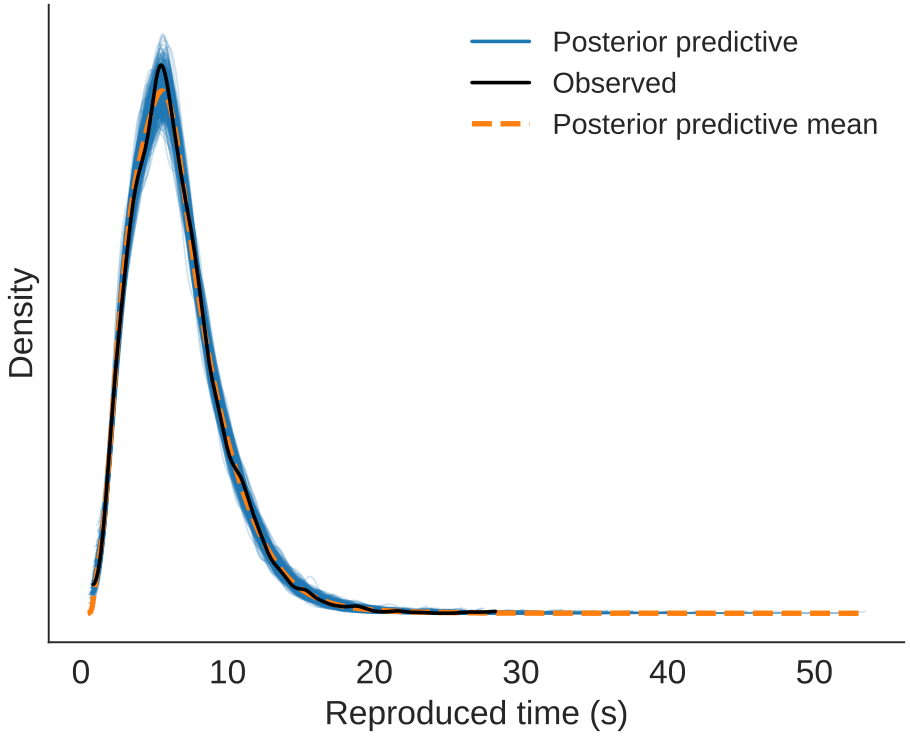


**Figure S4.** Wald model posterior predictive check. The observed distribution of reproduced times (black) is compared with 500 posterior predictive draws (blue). The orange dashed line represents their mean posterior predictive density.

## Quantile-Quantile analysis of reproduced times

To evaluate the goodness-of-fit of the WM, we extracted the best-fitting parameters for each participant (posterior means) from both the DDM and the WM and simulated the entire experiment once. Specifically, for each trial, we first simulated the drift-diffusion process underlying the choice between the two lotteries presented in that trial. The resulting RT and IT were then used as inputs to the WM to simulate the reproduced time. For each participant, we computed the 10th, 30th, 50th, 70th, and 90th quantiles of the simulated reproduced times and plotted them against the corresponding observed quantiles. As shown in Fig. S5, the WM provides a good fit to the observed data.

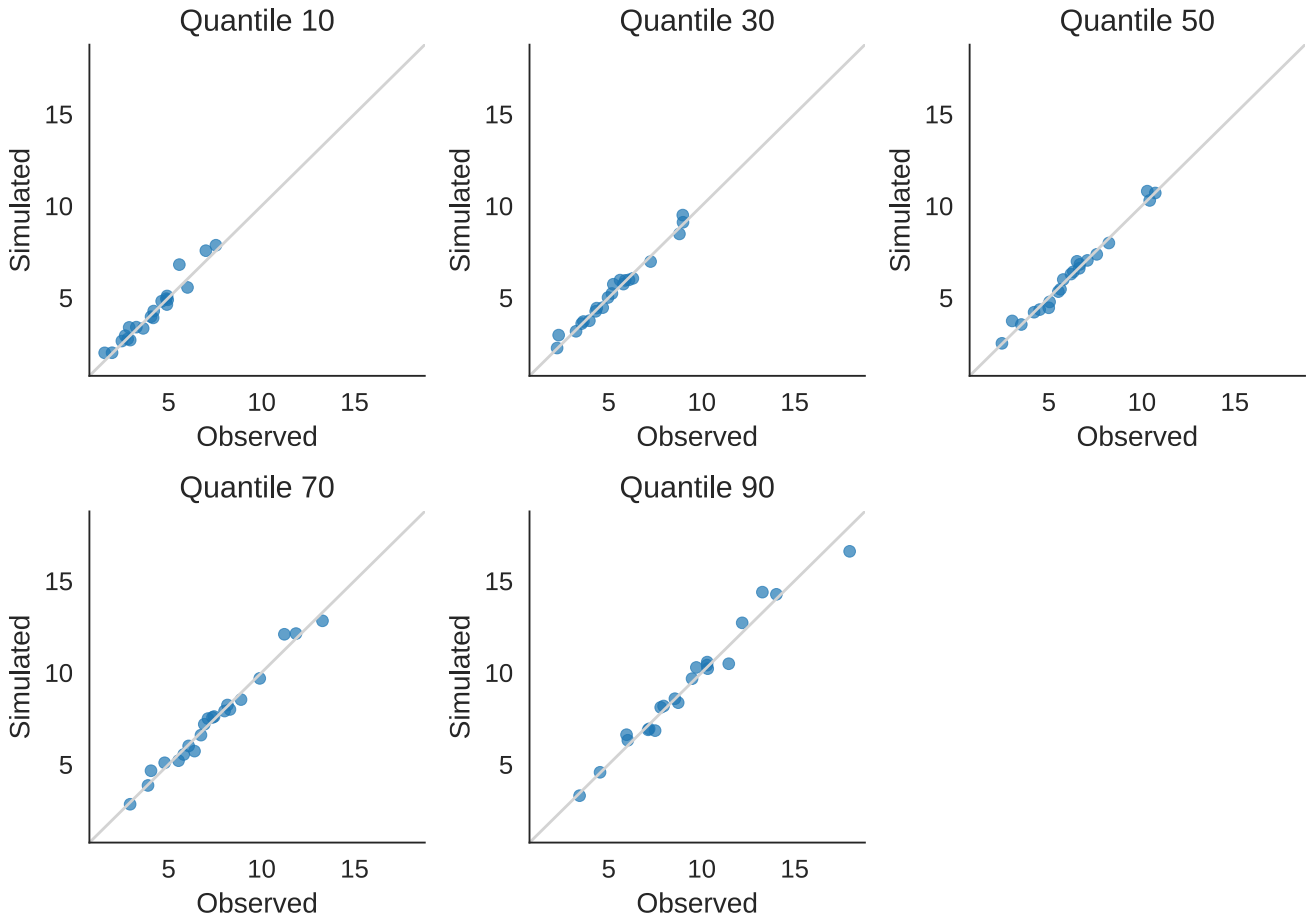


**Figure S5.** Quantile–quantile plot of observed versus simulated reproduced times for the Wald model. All axes are in seconds. The grey diagonal line indicates a perfect fit between observed and simulated values.

## Group-level parameter estimates of the Wald model

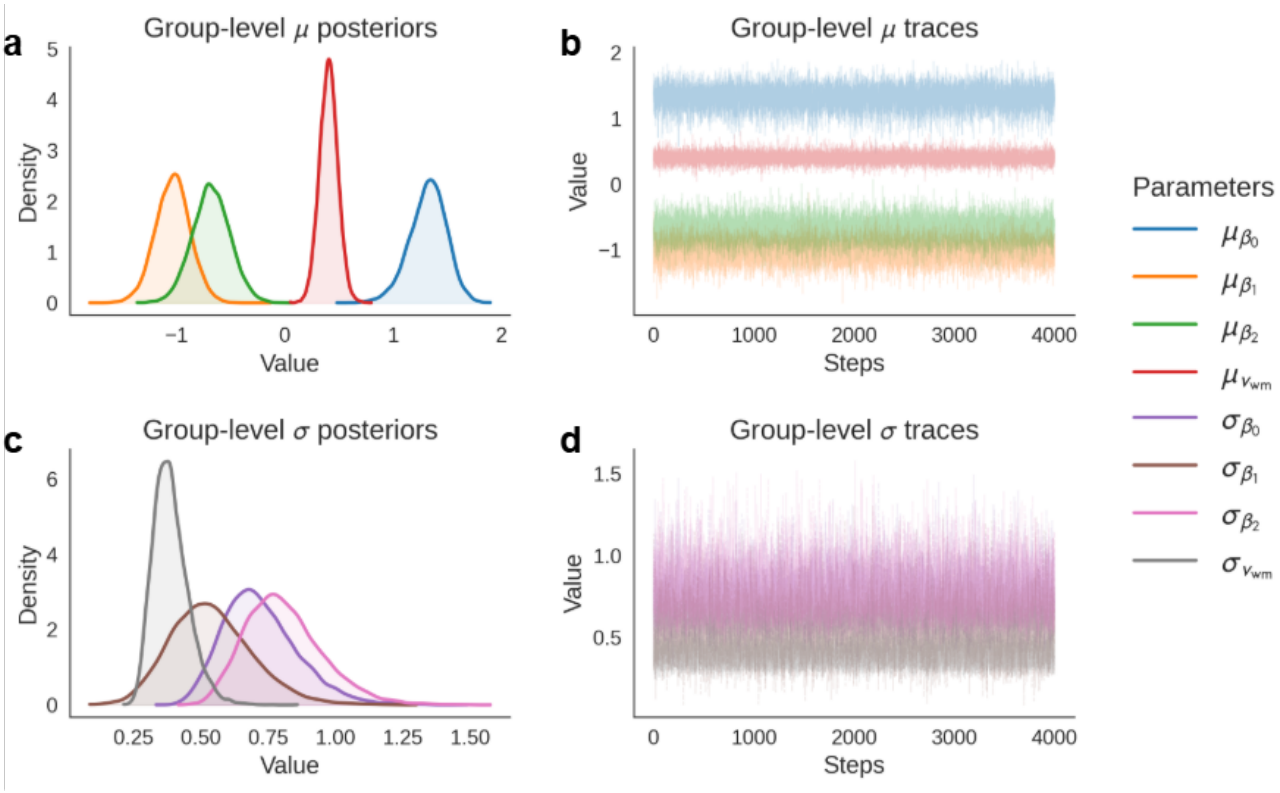


**Figure S6.** Group-level parameter estimates of the Wald model. (**a**, **b**) Posterior distributions and corresponding MCMC traces (after tuning) of the group-level means ($\mu_{\beta_0}$, $\mu_{\beta_1}$, $\mu_{\beta_2}$, and $\mu_{\nu_{wm}}$). (**c**, **d**) Posterior distributions and corresponding MCMC traces (after tuning) of the group-level standard deviations ($\sigma_{\beta_0}$, $\sigma_{\beta_1}$, $\sigma_{\beta_2}$, and $\sigma_{\nu_{wm}}$). All parameters showed good convergence, with $\hat{R} = 1$.

**Table S1.** Transformed group-level parameter estimates of the Wald model. For better interpretability, the group-level parameter estimates of the Wald model are reported after applying an exponential transformation ($\mu' = \exp(\mu)$ and $\sigma' = \exp(\sigma)$).

| Parameter | M | SD | HDI 3% | HDI 97% | $\hat{R}$ |
|---|---|---|---|---|---|
| $\mu'_{\beta_0}$ | 3.80 | 0.64 | 2.60 | 5.00 | 1 |
| $\sigma'_{\beta_0}$ | 2.08 | 0.31 | 1.56 | 2.63 | 1 |
| $\mu'_{\beta_1}$ | 0.36 | 0.06 | 0.25 | 0.47 | 1 |
| $\sigma'_{\beta_1}$ | 1.74 | 0.28 | 1.26 | 2.27 | 1 |
| $\mu'_{\beta_2}$ | 0.51 | 0.09 | 0.34 | 0.68 | 1 |
| $\sigma'_{\beta_2}$ | 2.27 | 0.35 | 1.71 | 2.91 | 1 |
| $\mu'_{\nu_{wm}}$ | 1.50 | 0.13 | 1.26 | 1.74 | 1 |
| $\sigma'_{\nu_{wm}}$ | 1.47 | 0.01 | 1.31 | 1.66 | 1 |

## Individual-level parameter estimates of the Wald model

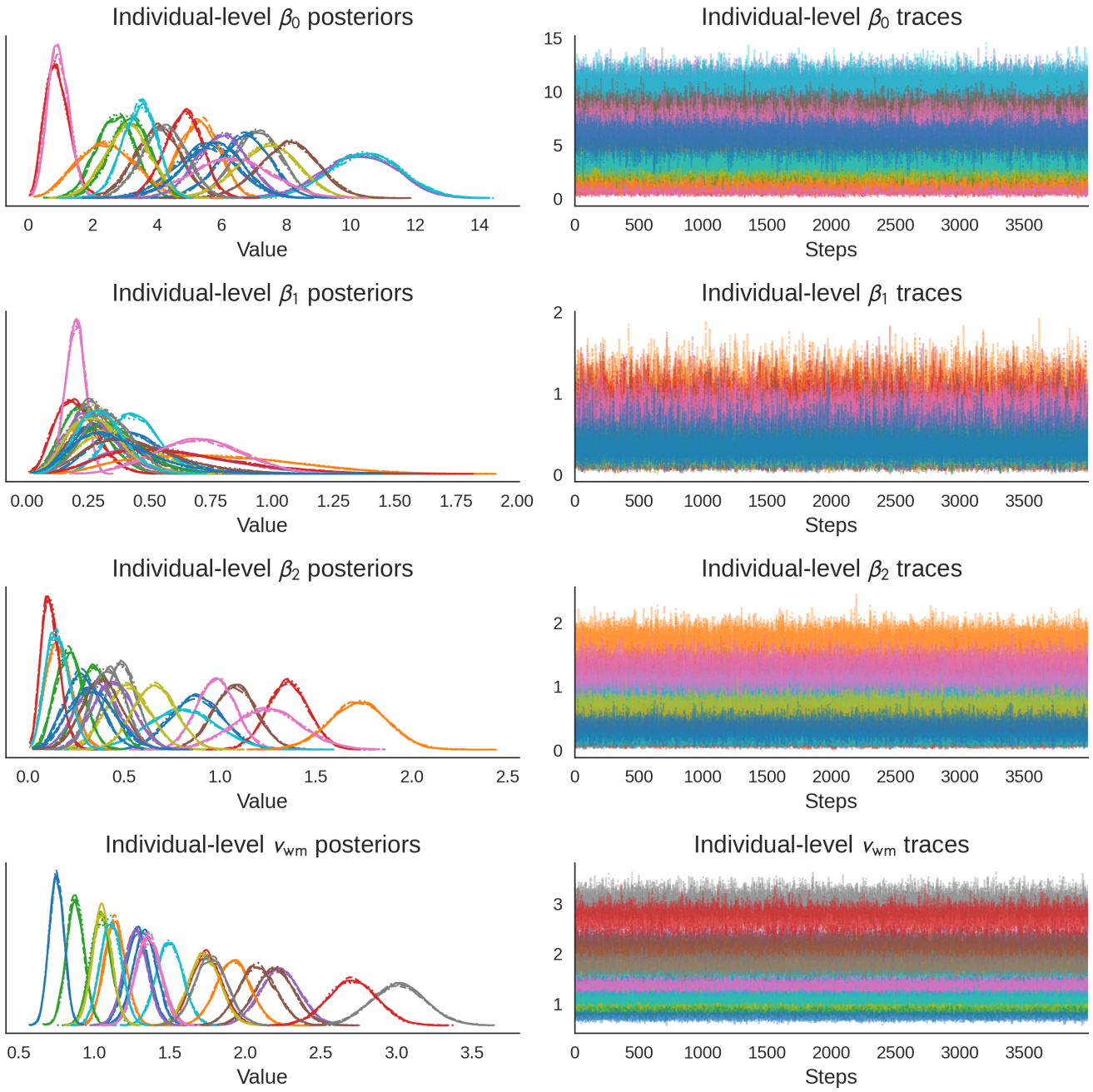


**Figure S7.** Individual-level parameter estimates of the Wald model. The plots on the left show the posterior distributions of the individual-level parameters of the Wald model. The plots on the right display the corresponding MCMC traces (after tuning). Each colour represents a different participant. All parameters showed good convergence, with $\hat{R} = 1$.

## Parameter estimates of the Drift-Diffusion model

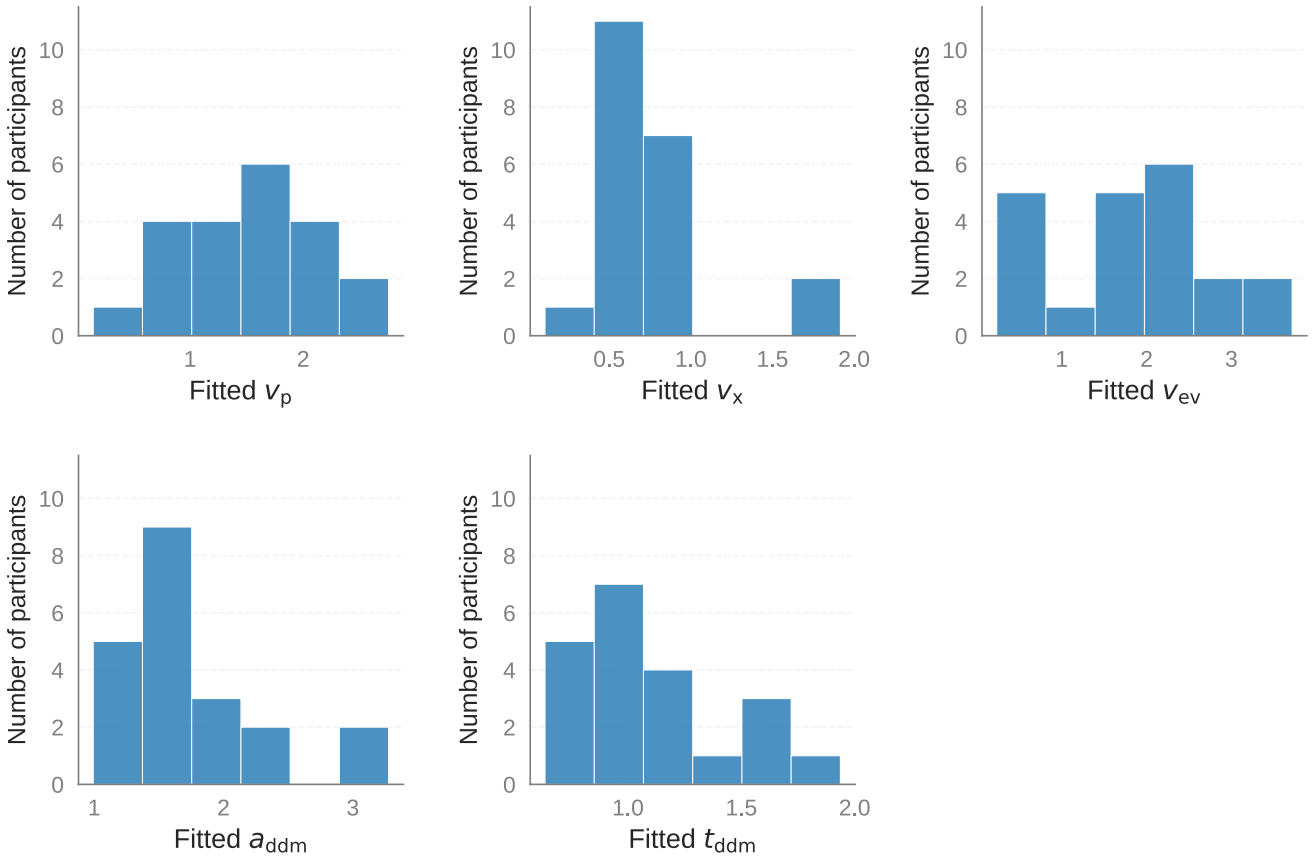


**Figure S8.** Posterior mean estimates of the parameters of the Drift Diffusion Model (DDM). The drift rate component associated with probability ($v_p$) tends to be larger than that associated with payoff ($v_x$), reflecting the greater proportion of participants who are risk-averse compared to risk-seeking, typically reported in the literature [26].

## Model comparison results

**Table S2.** Model comparison results. The table reports the best-fitting model rank, the estimated leave-one-out cross-validation score (elpd_loo) along with the standard error of this estimate (se), the difference in the score (elpd_diff) with respect to the score of the best-fitting model (i.e., the full Wald model), and the standard deviation of this difference (dse).

| Model | rank | elpd_loo | se | elpd_diff | dse |
|---|---|---|---|---|---|
| Full_wald | 1 | -6061.52 | 51.86 | 0.00 | 0.00 |
| Simple_wald | 2 | -6147.52 | 51.69 | 86.00 | 14.43 |
| Full_reg | 3 | -6236.57 | 58.48 | 175.05 | 21.41 |
| Simple_reg | 4 | -6331.29 | 58.37 | 269.78 | 25.26 |
| Null_wald | 5 | -6416.08 | 49.27 | 354.44 | 26.39 |

## Parameter recovery analysis

A parameter recovery analysis was conducted for the Hierarchical Bayesian Wald model and the Drift-Diffusion Model.

We first sampled 30 group-level Wald model parameter sets from the posterior distributions. For each group-level parameter set, 21 individual-level Wald model parameter sets were then sampled (equal to the number of participants in the study) from normal distributions parameterized by the means and standard deviations of the respective group-level parameters. In addition, for each individual-level parameter set, we included a corresponding DDM parameter set, sampled from uniform distributions with ranges approximately matching those of the estimated DDM parameters. Specifically, the DDM parameters were sampled from: $a_{\text{ddm}} \sim \mathcal{U}(0.5, 3.5)$, $t_{\text{ddm}} \sim \mathcal{U}(0.2, 2)$, $v_x \sim \mathcal{U}(0, 4)$, $v_p \sim \mathcal{U}(0, 4)$ and $v_{ev} \sim \mathcal{U}(0, 4)$.

For each combination of group- and individual-level parameters, we simulated the entire experiment using the same number of trials and stimuli as in the behavioural data, generating 30 synthetic datasets in total. Both models were then fitted to each of these datasets to recover both group- and individual-level parameters.

All individual-level parameters of the Wald and Drift-diffusion models were successfully recovered (Figs. S9 and S11, respectively). The group-level Wald model parameters were moderately recovered (Fig. S10), with stronger correlations for the means ($\mu_{\beta_0}$, $\mu_{\beta_1}$, $\mu_{\beta_2}$ and $\mu_{v_{\text{wm}}}$; Pearson's r = 0.68 – 0.76) compared to the standard deviations ($\sigma_{\beta_0}$, $\sigma_{\beta_1}$, $\sigma_{\beta_2}$ and $\sigma_{v_{\text{wm}}}$; Pearson's r = 0.54 – 0.67). The analysis also revealed that $\mu_{\beta_0}$ tends to be underestimated, whereas $\mu_{\beta_1}$ tends to be overestimated.

To examine potential trade-offs among Wald model parameters, we generated pairplots for all combinations of group- and individual-level parameter posterior means. Visual inspection of these plots (Figs. S12 and S13) suggests that the recovered parameters are not correlated and, therefore, that there are no evident trade-offs.

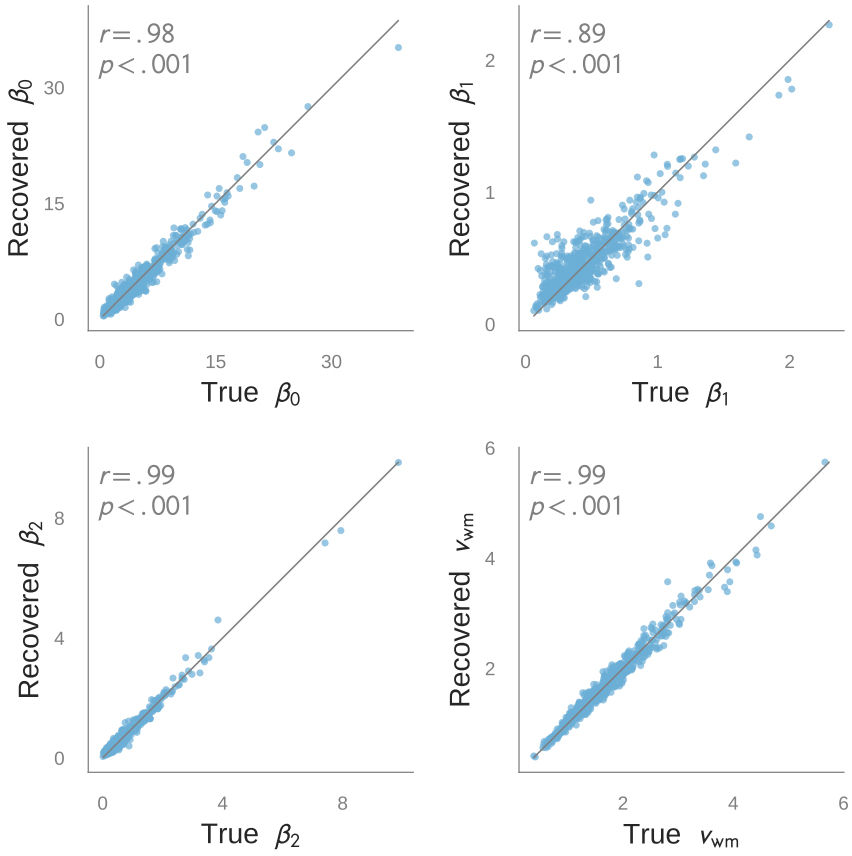


**Figure S9.** Individual-level parameter recovery for the Wald model. The plots show the estimated individual parameters (posterior means) plotted against the true generating parameters. The plots show the recovered parameters from 30 synthetic dataset simulations, each corresponding to a different group-level parameter set. The grey diagonal line indicates a perfect fit between true and recovered parameters. Pearson correlation coefficients ($r$) and their associated $p$-values (Bonferroni-corrected) are reported in the top-left corner of each plot. Bonferroni correction was applied by multiplying each original p-value by the number of Wald model parameters (12 in total, comprising both individual- and group-level parameters), which also corresponds to the number of statistical tests conducted.

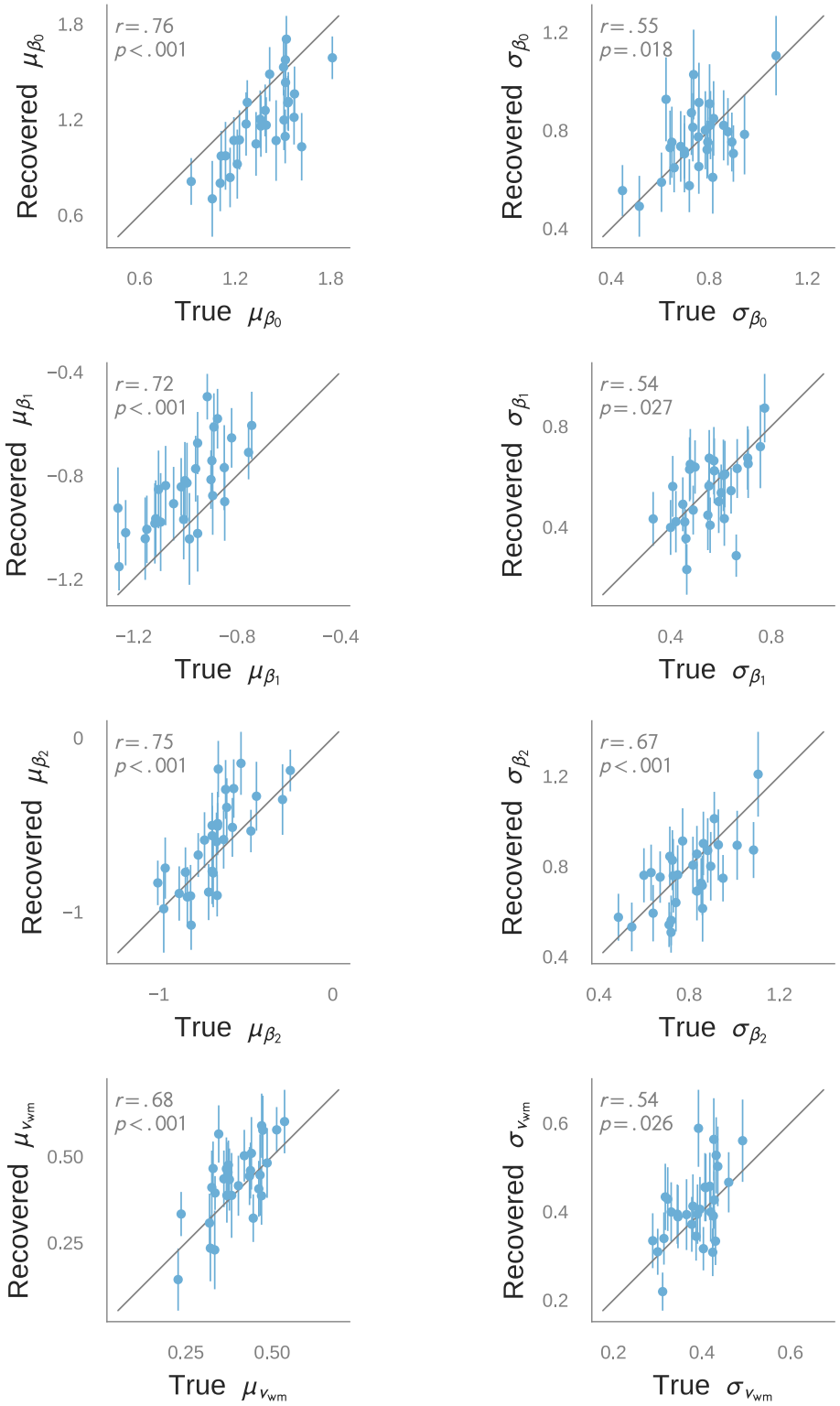


**Figure S10.** Group-level parameter recovery for the Wald model. The plots show the estimated group-level parameters (posterior means) with their corresponding posterior standard deviations, plotted against the true generating parameters. The grey diagonal line indicates a perfect fit between true and recovered parameters. Pearson correlation coefficients ($r$) and their associated $p$-values (Bonferroni-corrected) are reported in the top-left corner of each plot. Bonferroni correction was applied by multiplying each original p-value by the number of Wald model parameters (12 in total, comprising both individual- and group-level parameters), which also corresponds to the number of statistical tests conducted.

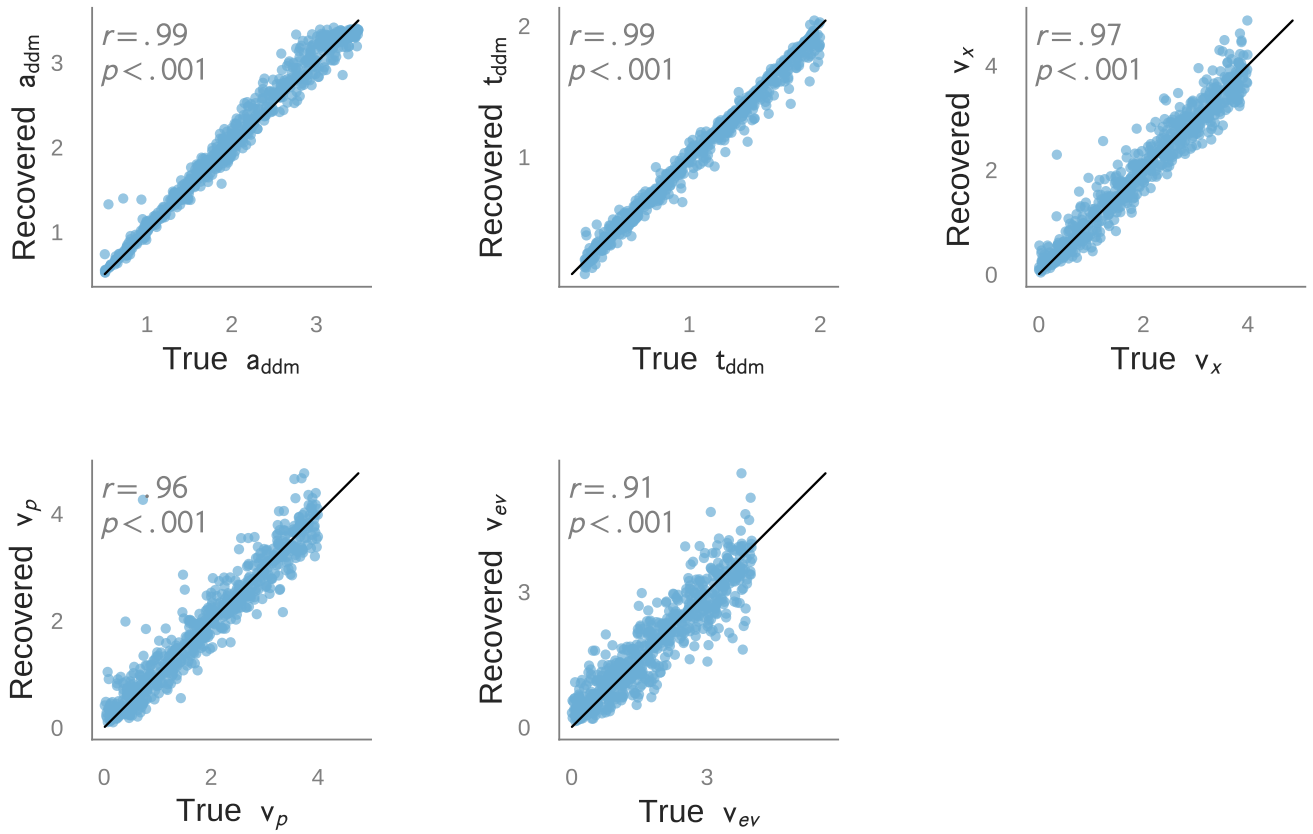


**Figure S11.** Parameter recovery for the Drift-diffusion model. The plots show the estimated parameters (posterior means), plotted against the true generating parameters. The plots show the recovered parameters from 30 synthetic dataset simulations. The black diagonal line indicates a perfect fit between true and recovered parameters. Pearson correlation coefficients ($r$) and their associated $p$-values (Bonferroni-corrected) are reported in the top-left corner of each plot. As for the Wald model recovery analysis, Bonferroni correction was applied by multiplying each original p-value by the number of DDM parameters (5 in total), which also corresponds to the number of statistical tests conducted.

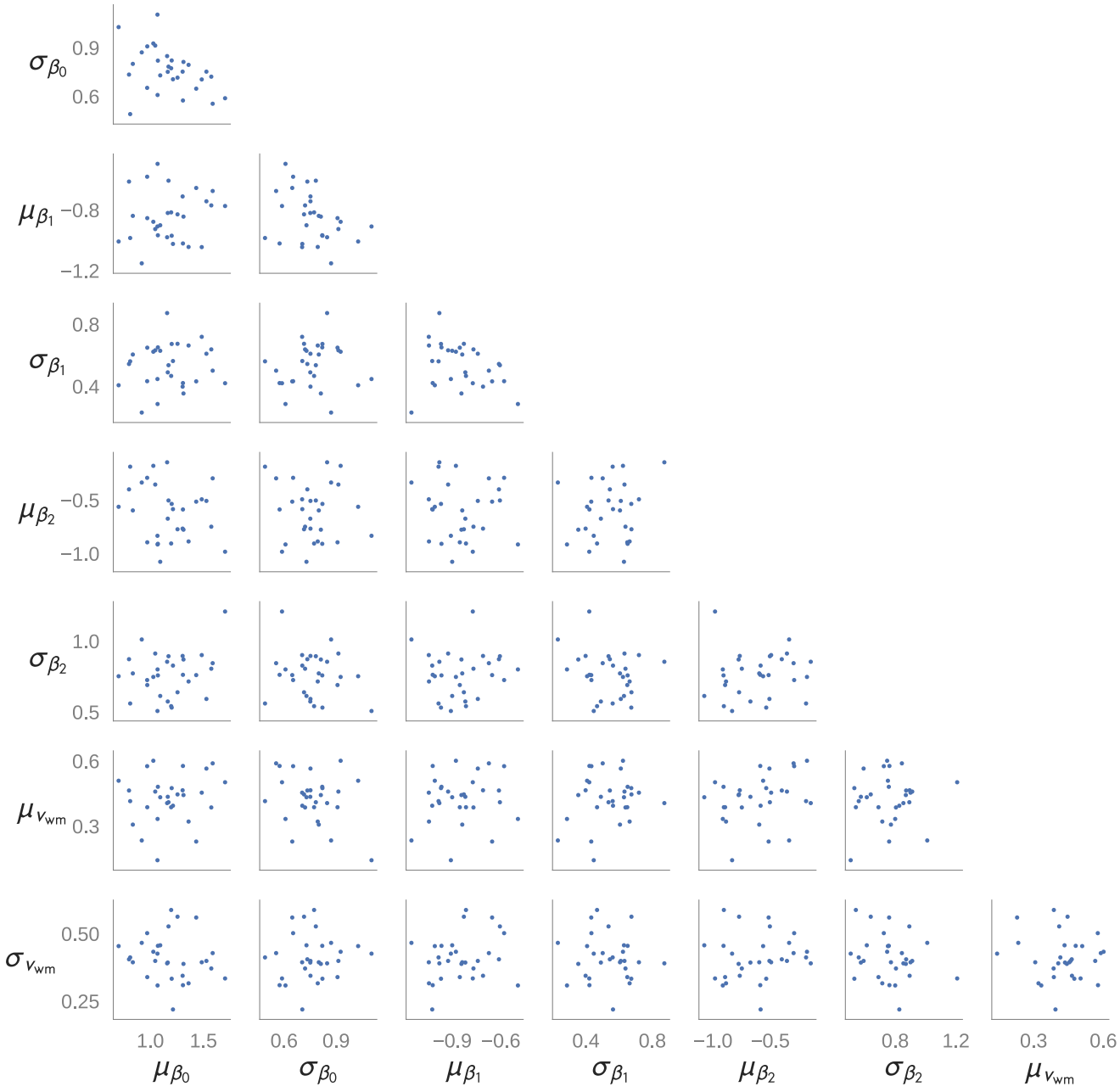


**Figure S12.** Pairwise scatter plots of recovered group-level Wald model parameters. No correlations were observed among any parameter combinations, suggesting that there are no trade-offs among the group-level parameters.

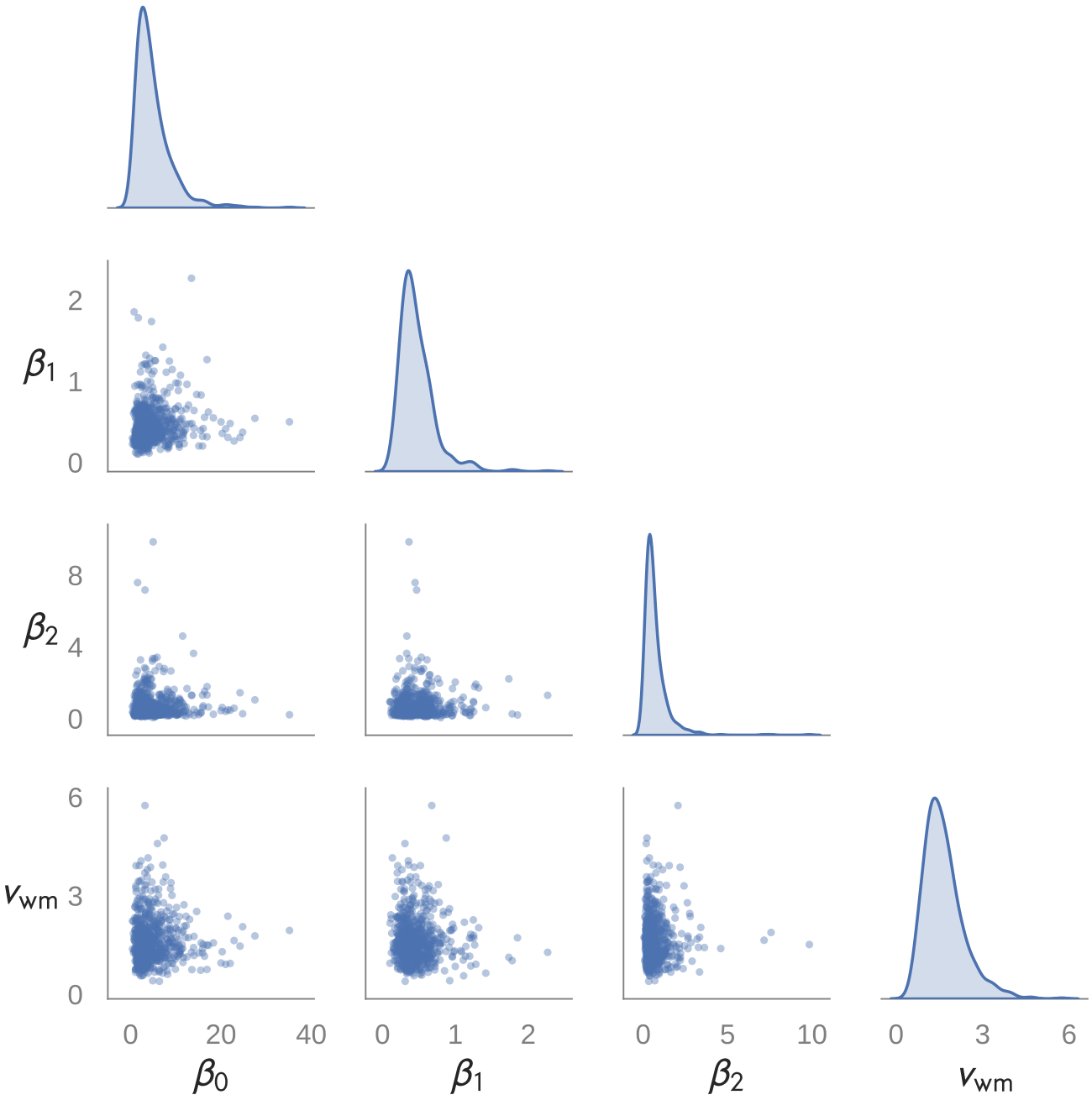


**Figure S13.** Pairwise scatter plots and posterior mean distributions of recovered individual-level Wald model parameters. The plots show the recovered parameters from 30 synthetic dataset simulations, each corresponding to a different group-level parameter set. As for the group-level parameters, no correlations were observed among any parameter combinations, suggesting that there are no trade-offs among the individual-level parameters.

## Mixed-effects models

**Table S3.** Summarised results of mixed-effects models. For the linear mixed-effects models (lme_1, lme_2, lme_3, and lme_4), p-values for fixed effects were obtained using two-tailed t-tests of the null hypothesis that the corresponding regression coefficients equal zero, with Satterthwaite-approximated denominator degrees of freedom as implemented in the *lme4*[42] package. For the cumulative link mixed models (clm_null, clm, clm_s), p-values for fixed effects were obtained using likelihood ratio tests (LRTs) comparing the full model containing the fixed effect to the same model without that effect. Models marked with (*) were fitted on the same data used to fit the DDM; all other models used the same data as the rest of the analyses of the study, as described in the Data Pre-processing section. Categorical fixed-effects are denoted with c(). Here, "Subj" refers to participants, and "$\text{SubjDiff}_3$" to the participants' subjective difficulty ratings, where the categories "Very easy" and "Easy" were binned together into a single "Easy" category and "Very hard" and "Hard" were binned together into a single "Hard" category, resulting in three levels of subjective difficulty. The coefficients of all the fixed effects are reported with standard errors in brackets.

| Name | Formula | Fixed-effect coefficients ($\beta$) | Significance | $R^2_m$ |
|---|---|---|---|---|
| lme_1* | $\log(RT) \sim (1 \mid Subj) + dX_z + dP_z + dX_z * dP_z$ | $dX_z$: −0.099 (0.006)<br>$dP_z$: −0.072 (0.006)<br>$dX_z * dP_z$: −0.046 (0.006) | $t(3270) = -16.486$, $p < 0.001$<br>$t(3270) = -12.884$, $p < 0.001$<br>$t(3270) = -7.836$, $p < 0.001$ | 0.037 |
| clm_null* | $\text{SubjDiff}_3 \sim 1 + (1 \mid Subj)$ | | | |
| clm* | $\text{SubjDiff}_3 \sim (1 \mid Subj) + \log(RT)$ | log(RT): 2.578 (0.135) | LRT(clm, clm_null):<br>$\chi^2(1) = 418.121$, $p < 0.001$ | |
| clm_s* | $\text{SubjDiff}_3 \sim (1 \mid Subj) + \log(RT)$<br>(scale = ∼ log(RT)) | log(RT): 2.302 (0.158)<br>log(RT) (scale): −0.148 (0.059) | LRT(clm, clm_s):<br>$\chi^2(1) = 6.165$, $p = 0.013$ | |
| lme_2 | $\log(DJR) \sim (1 \mid Subj) + \frac{RT}{TT} + c(TT)$ | $\frac{RT}{TT}$: −0.294 (0.037)<br>c(TT) (8 s): −0.177 (0.013)<br>c(TT) (10 s): −0.312 (0.014) | $t(3254.640) = -7.892$, $p < 0.001$<br>$t(3237.862) = -13.560$, $p < 0.001$<br>$t(3241.583) = -22.669$, $p < 0.001$ | 0.066 |
| lme_3 | $\log(DJR) \sim (1 + \frac{RT}{TT} \mid Subj) + \frac{RT}{TT} + c(TT)$ | $\frac{RT}{TT}$: −0.254 (0.141)<br>c(TT) (8 s): −0.169 (0.013)<br>c(TT) (10 s): −0.300 (0.014) | $t(18.781) = -1.801$, $p = 0.088$<br>$t(3232.281) = -13.205$, $p < 0.001$<br>$t(3237.206) = -21.930$, $p < 0.001$ | 0.066 |
| lme_4 | log(ReproT) ∼ (1 + TT \| Subj) + TT | TT: 0.060 (0.009) | $t(20.057) = 6.589$, $p < 0.001$ | 0.039 |

Table S3 summarises the results of the fitted cumulative link mixed models (clm_null, clm, and clm_s) and linear mixed-effects models (lme_1, lme_2, lme_3, and lme_4).

To simplify the analysis of how subjective difficulty ratings depended on reaction times (RTs), we recoded the original Likert scale by binning the categories "Very easy" and "Easy" into a single "Easy" category, and "Very hard" and "Hard" into a single "Hard" category, resulting in three levels of subjective difficulty. This recoded variable ($\text{SubjDiff}_3$) served as the dependent variable in all cumulative link mixed models. In addition, we found that using log-transformed RT as a fixed effect, rather than raw RT, provided a better fit to the data. In terms of AIC, comparing the clm model with log(RT) to the same model with raw RT as a fixed effect resulted in $\Delta AIC = -25.115$, in favour of the log(RT) model.

For the cumulative link models, the proportional odds assumption[48] was tested with a likelihood ratio test (LRT) comparing the clm model to the same model including nominal effects for log(RT) (in the *ordinal*[47] package, setting *nominal* = ∼ *log(RT)*). The result suggested that the proportional odds assumption holds ($\chi^2(2) = 0.999$, $p = 0.607$). We also tested whether including scale effects dependent on log(RT) improved model fit. This was done via an LRT comparing the clm model to the same model including scale effects for log(RT) (in the ordinal package, setting *scale* = ∼ *log(RT)*). The result (reported in Table S3) indicated that including scale effects led to a better fit ($\chi^2(1) = 6.165$, $p = 0.013$). The coefficient of the scale effect was negative ($\beta = -0.148$ (SE = 0.059)), indicating that when log(RT) is higher (i.e., decisions are slower), participants are more consistent in how difficult they perceive those trials to be (i.e., there is less variability in their difficulty ratings).

To report effect sizes for the clm_s model (which was the best-fitting), we could not rely on the marginal $R^2_m$, since it cannot be computed for cumulative link mixed models. Although it is possible to calculate pseudo-$R^2$ through various methods, we

opted for a more interpretable test, namely calculating the odds ratio[48] for the log(RT) effect. The odds ratio can be interpreted as the ratio of the odds of being in a given category or greater given a specific value of the independent variable ($x_1$) and the odds of being in a given category or greater given another particular value of the independent variable ($x_2$). The odds ratio (OR) is then given by:

$$\mathrm{OR} = \exp[(x_2 - x_1)\hat{\beta}]$$

Where $\hat{\beta}$ is the (mean estimate) coefficient of the fixed effect of interest obtained when fitting the cumulative link mixed model, and as mentioned earlier $x_1$ and $x_2$ are two values of the independent variable that we want to compare. In our case, we are interested in the odds ratio associated with doubling the RT. Hence, setting $x_1$ = log(RT) and $x_2$ = log(2 RT) (i.e., doubling the RT) results in:

$$\mathrm{OR} = \exp\{[\log(2\mathrm{RT}) - \log(\mathrm{RT})]\hat{\beta}\} = \exp[\log(2)\hat{\beta}]$$

Plugging in the mean estimated coefficient ($\hat{\beta} = 2.302$), the resulting odds ratio is equal to OR $\approx 4.931$. To calculate the confidence intervals, we assume a normal distribution for the parameter estimate such that the confidence interval is given by $\mathrm{CI} = \hat{\beta} \pm 1.96 \cdot \mathrm{SE}_\beta$ (where $\mathrm{SE}_\beta$ is the standard error of the parameter estimation). Hence, we can estimate CIs for the OR as follows:

$$\mathrm{OR} = \exp\{\log(2)(\hat{\beta} \pm 1.96 \cdot \mathrm{SE}_\beta)\} = [3.981, 6.112]$$

For all linear mixed-effect models, we compared each tested model to simpler nested models with fewer fixed effects using AIC scores. All tested models (lme_1, lme_2, lme_3, and lme_4), achieved lower AIC values than their simpler versions. In addition, visual inspection of residuals and random intercepts indicated approximate normality, minor to no heteroscedasticity in the residuals, and no evidence of multicollinearity among the fixed effects. All these analyses can be reproduced using the code we have made publicly available.

## Supplementary Table S4

**Table S4.** Per-participant Bayesian Credible Intervals (BCIs) for $\beta'_1 < \beta'_2$. For each participant, we computed the posterior distribution of $\beta'_1 - \beta'_2$ and estimated the posterior probability mass below zero (corresponding to $\beta'_1 < \beta'_2$.) Rows with a BCI greater than 95% are shown in green.

| Participant ID | $\beta'_1 < \beta'_2$ BCI |
|---|---|
| 1 | 99.95% |
| 2 | 7.93 % |
| 3 | 84.88 % |
| 4 | 100.00 % |
| 5 | 17.23 % |
| 6 | 100.00 % |
| 7 | 100.00 % |
| 8 | 99.22 % |
| 9 | 80.02 % |
| 10 | 99.47 % |
| 11 | 42.28 % |
| 12 | 99.78 % |
| 13 | 14.76 % |
| 15 | 0.38 % |
| 16 | 91.36 % |
| 17 | 40.58 % |
| 18 | 100.00 % |
| 20 | 83.15 % |
| 21 | 99.54 % |
| 22 | 6.49% |
| 23 | 46.86 % |

## Relationship between $\beta'_0$ and the central tendency bias

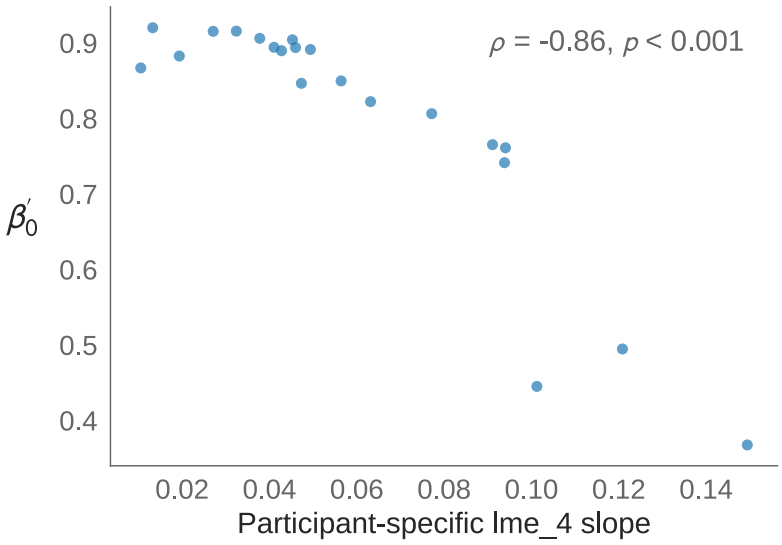


**Figure S14.** Participant-specific estimated $\beta'_0$ plotted against the participant-specific slopes from the lme_4 linear mixed-effects model. A smaller slope is associated with a greater central tendency bias. Spearman's rank correlation, along with the p-value, is shown in the upper-right corner.

## Evolution of the Coefficient of Variation as a function of target time for the Wald model

For simplification, assuming that the pulse accumulation rates are equal during decision-making and idle phases (i.e. $\beta_1 = \beta_2$), then the mean ($\mu$), and standard deviation ($\sigma$) of the reproduced times for the WM are given by the following equations:

$$\mu = \frac{\alpha}{v_{\text{wm}}} = \frac{\beta_0 + \beta_{\text{time}}\text{TT}}{v_{\text{wm}}} \tag{1}$$

$$\sigma = \sqrt{\frac{\alpha}{v_{\text{wm}}^3}} = \sqrt{\frac{\beta_0 + \beta_{\text{time}}\text{TT}}{v_{\text{wm}}^3}} \tag{2}$$

Where $\beta_{\text{time}} \coloneqq 2\beta_1 = 2\beta_2$ and $\text{TT} = \text{RT} + \text{IT}$ is the target time to be reproduced.

Given equations (1) and (2), we can show that the coefficient of variation (CV) decreases with target time following this relationship:

$$\text{CV} = \frac{\sigma}{\mu} = \frac{1}{\sqrt{v_{\text{wm}}(\beta_0 + \beta_{\text{time}}\text{TT})}} \propto \frac{1}{\sqrt{\text{TT}}} \tag{3}$$

Interestingly, if we no longer assume that pulse-transfer rates are the same during decision-making as during idleness (i.e., $\beta_1 \neq \beta_2$), then the WM also predicts that participants with a higher central tendency bias will show less variation in CV as the deadline increases, since their "time representations" are more constant across deadlines, when compared to the rest of the participants. However, we found no evidence supporting this prediction.